RSC Advances

PAPER

View Article Online
View Journal | View Issue

Cite this: *RSC Adv.*, 2024, **14**, 37380

Active packaging films based on the nanoform of chitin, alginate, and layered double hydroxides: characterization, mechanical properties, permeability, and bioactive properties

Mohamed S. Hasanin, *[a] Youssef R. Hassan[b] and Ahmed M. Youssef[bc]

Their unique characteristics make plastic films frequently utilised for packaging products. However, this petroleum-derived material has a long history of being linked to environmental contamination and hazardous degradation. Petroleum plastic can be substituted with edible packaging. The objective of this study was to combine sodium alginate with chitin, both in their nanosized form to formulate active packaging films containing different ratios of Zn/Al-layered double hydroxides (LDHs). Subsequently, active packaging films were formulated *via* a green method with different percentages (0%, 1%, 3%, and 5% w/w) of LDHs. The LDH particles were shaped as rectangular rods with a length of about 60 nm and width of around 20 nm. The films were evaluated for their physicochemical, topological, thermal, mechanical, water vapour, oxygen permeability and antimicrobial properties. Results indicated that active packaging with LDHs (3%) enhanced mechanical properties (tensile strength) by two-fold. Moreover, the addition of LDHs led to decreased permeability properties. Additionally, the antimicrobial study showed that the films with LDHs possessed a broad spectrum of antibacterial and antifungal activities, and the time required for bacterial killing was recorded to be less than 16 hours for films containing 5% LDHs. Thus, the formulated films show potential for use as active packaging.

Received 1st September 2024
Accepted 5th November 2024

DOI: 10.1039/d4ra06306f

rsc.li/rsc-advances

Introduction

The food shortage is a dangerous condition, causing deaths around the world.[1] In this context, the United States Department of Agriculture (USDA) has defined food insecurity as a lack of dependable access to enough food for everyone.[2] Moreover, according to the World Health Organization (WHO), more than two hundred diseases can be transmitted through contaminated food, resulting in 420 000 deaths and the loss of 33 million healthy lives per year.[3]

Generally, food and health associations use hunger and food insecurity to represent the lack and contamination of food. Accordingly, active packaging materials can preserve food and prevent hunger.[4–6] Various petroleum-based polymer packaging materials, such as high-density polyethylene (HDPE), low-density polyethylene (LDPE), polypropylene (PP), polyethylene terephthalate (PET), and acrylonitrile butadiene styrene (ABS), still dominate the food packaging sector owing to their high mechanical properties, flexibility, and low cost but are biodegradable during transport.[7–9] Consequently, in recent years, food contamination with plastic ingredients has become a global problem, posing a serious threat to consumer health and environmental pollution.[10,11]

Alternatively, biopolymers play a restricted role in food packaging applications despite their excellent salient features, including environmentally friendly nature, biodegradability, and biocompatibility.[12–14] However, some of them lack the biological activity to overcome the issue of contaminants. Indeed, biopolymers loaded with bioactive materials lead to an amplification of the properties of these multifeatured materials.[5,15] In addition, alginates are natural polysaccharides extracted from some marine brown algae with chemical structures composed of linear homopolymeric (D-mannuronic acid (M block) and L-guluronic acid (G block)) and heteropolymeric regions (M blocks and G blocks), which are anionic radicals usually used as a sodium salt and are nontoxic and approved by the FDA .[16,17] Meanwhile, the sodium salt of alginate is a water-soluble polysaccharide that is characterised by biological compatibility. However, the viscosity of alginate solution is not adequate for the formulation of films; thus, they sometimes need support from other materials.[18,19] Compared to cellulose, which is the most prevalent polysaccharide in nature, chitin may be the second most prevalent.[20] Chitin is a long-chain polymer of *N*-acetylglucosamine, an amide derivative of glucose, and is the

[a]*Cellulose and Paper Department, National Research Centre, 12622, Dokki, Cairo, Egypt. E-mail: sido_sci@yahoo.com*

[b]*Packaging Materials Department, National Research Centre, 12622, Dokki, Cairo, Egypt*

[c]*Electronics Research Institute (ERI), Joseph Tito St, Huckstep, El Nozha, Cairo Governorate 4473221, Egypt*

source of chitosan. Alternatively, nanochitin is one of the new nanomaterials reported to show unique properties, including strong biological activities and low toxicity, for application in the biomedical, agriculture, and food packaging fields.[21–23] Accordingly, nanochitin can be employed to support low viscosity film formulation components.

Nanometals have numerous uses as well as added multifunction properties, which can be used in active packaging materials.[24] Among them, layered double hydroxides (LDHs) such as aluminium oxide/zinc oxide are advanced and unique nanomaterials. LDHs have attracted significant attention in recent years due to one of their key features of surface protection, together with their advantages of mass production and potential productivity.[25,26] LDHs are used in packaging films as additive materials in low concentrations to enhance their barrier, mechanical, and thermal properties.[27–30] Furthermore, LDHs possess abundant hydroxyl groups, adding to the biological advantages of these metal oxides.[31] Therefore, in this study, we explored the possibility of using nanoscale sodium alginate and chitin as renewable resources to prepare cross-linked films doped with layered double hydroxides (LDHs), possessing the additional advantages of improved thermal and food active packaging properties. Additionally, the produced active packaging films were characterized physiochemically, topographically, mechanically, and biologically. In this context, the present study aims to fill the gap in active packaging by delving deeper into the characterization, properties, and potential applications of the prepared films.

Materials and methods

Materials

Sodium alginate (SA) was supplied from Alpha-Chemika (India). Glycerol (Gl) and tannic acid (CA) were obtained from Merck Company (Germany) and used without further purification. Chitin purified flakes (molecular formula: $(C_8H_{13}\ NO_5)_n$) with a nitrogen content of 6.0–8.0% was obtained from SDFCL Co., Mumbai, India. For the preparation of 2 : 1 ZnAl LDH, Zn-acetate ($C_4H_6O_4Zn\cdot 2H_2O$, puriss, Reanal, Hungary), Al-nitrate ($Al(NO_3)_3\cdot 9H_2O$, puriss, Molar, Hungary) and $NaNO_3$ (puriss, Reanal) precursors were used with NaOH (A.R., Molar, Hungary). All other organic solvents, as well as microbial media and reagents used in this study, were of analytical grade and used without further purification. They were purchased from Loba Chem Co., India.

Methods

Preparation of layered double hydroxide (Zn-Al LDH). The layered double hydroxide was synthesized according to the method reported in the literature.[32] Before its preparation, carbonate-free distilled water was obtained by boiling and N_2-bubbling through cooled water. In the case of the 2 : 1 composition, an Al-nitrate ($Al(NO_3)_3\cdot 9H_2O$) solution containing 37.5 g of solute and 600 mL of water was stirred in a three-neck round flask, and then Zn-acetate ($C_4H_6O_4Zn\cdot 2H_2O$) solution (43.8 g in 600 mL) was poured to the above-described solution. Then, a solution of NaOH (28.0 g) in excess and Na-nitrate (20.0 g) in 2800 mL of carbonate-free distilled water was slowly added (within 10 min) to the precursor-containing mixture under vigorous stirring and an N_2-atmosphere. The white dispersion was heated to 60 °C and left for 5 h. Subsequently, the precipitate was aged for 14 days at ambient temperature. The dispersion was centrifuged and washed, while the original pH of 9–10 decreased to 8–9. The washed samples were dried at 60 °C to obtain the final product.

Active packaging film formulation. The active packaging films were prepared using nanoalginate (sodium salt) (NALG) prepared according to ref. 33 and 34 and suspended in double-distilled water with a concentration of 3% (w/v). Nanochitin (NCH) was prepared according to ref. 35 and suspended at a concentration of 0.3% (w/v). Afterwards, both of the above-prepared suspensions were mixed (100 mL each) under vigorous stirring conditions for 4 h at 70 °C, and the mixture produced, called NALG/NCH, was divided into 50 mL. LDHs (1 g) were suspended in 100 mL double distilled water and ultrasonicated with an ultrasonic tip for 3 min. The LDHs were added with different concentrations to 50 mL of NALG/NCH individually as equivalent volumes for 0 (blank), 1%, 3%, and 5% w/w based on the solid content of the film constituents. The prepared mixtures were ultrasonicated in a water bath for 1 h at 70 °C. The active packaging films were cast in Teflon dishes with a diameter of 15 cm and depth of 5 mm and left to dry in an oven overnight at 70 °C. The formulated films were maintained at 23 ± 2 °C and relative humidity of 50 ± 5%.

LDH characterisation. The LDHs were characterised *via* surface morphological analysis on a field emission SEM, Model Quanta 250 FEG and TEM, Model JEM2010, Japan. Dry samples were used for the SEM analysis, whereas they were suspended in deionized water at a concentration of 0.1 g/5 mL for TEM.

Active packaging film characterization. The surface morphology and topography analysis was performed using SEM and TEM. The physiochemical analysis was performed on an FTIR spectrometer (Nicolet Impact-400 FT-IR spectrophotometer) in the range of 400–4000 cm^{-1}. X-ray diffraction (XRD) patterns were recorded using a Philips X-ray diffractometer (PW 1930 generator, PW 1820 goniometer) with a CuK radiation source ($\lambda = 0.15418$ nm). TGA was carried out using a TGA Q500 device.

Mechanical. Tensile strain testing was carried out according to the TAPPI T494-06 standard method using a universal testing machine (LR10K; Lloyd Instruments, Fareham, UK)[36] with a 100-N load cell at a constant crosshead speed of 2.5 cm min^{-1} including tensile strength (MPa), Young's modulus (MPa) and elongation at break (mm).

Permeability study. A GBPI W303 (B) water vapor permeability analyzer was employed to measure the water vapour transmission rate using the cup method. The water vapour transmission rate (WVTR) was calculated in terms of the amount of water vapour that moved in a unit of time across a unit area under a specific humidity of 4–10% and temperature of 38 °C according to the standards of JIS Z0208, 53122-1, TAPPI T464, ASTM D1653, ISO 2528, and ASTM E96. The rate of transmission of gas (GTR, O_2) was measured by using an N530 B

Gas Permeability Analyzer (China), according to the ASTM D1434-82 (2003) standards.

Antimicrobial study

Strains cultivated. Foodborne microorganisms were selected according to the main purpose of the presented work. The selected microbial strains used in the antimicrobial test were cultures of the following microorganisms: *Escherichia coli* (NCTC-10416), *Pseudomonas aeruginosa* (NCID-9016), *Streptococcus aureus* (NCTC-7447), *Bacillus subtilis* (NCID-3610), *Candida albicans* (NCCLS 11) and *Aspergillus niger*. The cultivation of bacteria was carried out on a nutrient medium, and unicellular fungi strains were cultivated on a potato dextrose broth medium. Unicellular fungi were cultivated for 24 h at 37 °C and filamentous fungi for 72 h at 27 °C, while the bacterial strains were grown in nutrient broth medium for 24 h at 37 °C. The turbidimetric method was used, according to our previous work.[37–39] The weight of the films (0.2 g) was defined, and they were suspended in the culture media after sterilisation using a UV-lamp 450.

Time required for killing. The time required for killing the microorganisms during exposure to the active packaging films was determined according to Eid, I. *et al.*, 2017.[40] The obtained data were compared with a blank sample that contained all the microorganisms without a test sample.

Statistical analysis. The results were expressed as the mean ± standard deviation for triplicate samples. The statistical analysis was performed using the XLSTAT 2014 (5.03) software (USA).

Results and discussion

LDHs characterization

The evaluation of the LDHs is illustrated in Fig. 1, which involved TEM and SEM imaging and FTIR spectroscopy. The TEM images with low magnification (Fig. 1a) showed that the LDH particles were arranged over each other with a type of condensation. Alternatively, the high-magnification image (Fig. 1b) illustrated the particle shape as rectangular rods with a length of about 60 nm and width of around 20 nm, which confirmed the nanosize of the LDHs and is in agreement with previous works.[41,42] Furthermore, the SEM images emphasised the surface morphology that appeared at low magnification (Fig. 1d) as a needle-like shape that looked like rectangular rods. In addition, the high-magnification SEM image (Fig. 1c) illustrated the LDH particles as an irregular surface with aggregated particles, which is in agreement with the previous works.[43–45] Notably, the difference in the details between the SEM and TEM images is due to the nature of the sample preparation method during the test.

The FTIR spectrum of LDHs (Fig. 1e) shows a broad band at about 3420 cm^{-1}. It is ascribed to the O–H stretching vibration in the interlamellar water molecules and brucite-like layers, whilst the hydrogen bond formation is responsible for its broadening.[46] The band at 1630 cm^{-1} indicates the bending vibration of the interlayer water molecules. The band at 1455 cm^{-1} corresponds to the symmetrical C=O stretching in the carboxyl group, and the bands at 1351 and 1189 cm^{-1} correspond to the C–O and C–O–C stretching in the acetyl group, respectively.[47,48] In summary, the above-mentioned results confirmed the successful formulation of LDHs. The XRD pattern of LDHs is illustrated in Fig. 1f. The diffraction peaks show a well-formed crystalline layered structure for the (003), (006), (012), (107), (015), (1010), (110) and (113) crystal planes, corresponding to the peaks at 2θ values of 11.34°, 23.77°, 35°, 36.2°, 52.05°, 63° and 68°, respectively, which show that the metal ions in the hydroxide layers are well dispersed according to the previous reports.[49,50]

Formulation of active packaging films

The film formulation active packaging films were based on the NALG reinforced with 10% NCH and loaded LDHs with three different concentrations of 0.1%, 0.3%, and 0.5% w/w. The hypothesis for the formulation of the active packaging films was based on the following aspects. Firstly, the active packaging films use NALG as the main matrix, which is edible, biodegradable, and nontoxic. Secondly, NCH was added in a fixed concentration (0.3% (w/v)) to increase the viscosity of the formulated film. Thirdly, LDHs were added as a suspension to achieve an excellent distribution in the film matrix. LDHs were added in different concentrations, namely 1%, 3%, and 5% w/w, based on the solid content of the film constituents and compared with the blank (NALG/NCH). A comparison study was carried out to investigate the efficiency of LDHs to act as a crosslinker according to their high content of hydroxyl groups and the enhancement of the mechanical, permeability, and antimicrobial properties.

Characterization of active packaging films

The characterization of the active packaging films was carried out *via* physiochemical and topographical analysis. The physiochemical analysis included FTIR (Fig. 2) and XRD (Fig. 3), which were used to study the difference between the neat materials and the formulated active packaging films. The FTIR spectrum of NALG in the nanoscale showed evident bands at 3377, 2942, 1614, 1413, and 1037 cm^{-1}, which are ascribed to the alginate functional groups such as hydroxyl groups stretching vibrations, CH_3 stretching vibrations, symmetric stretching vibrations of the carboxylic groups, and a symmetric and carbohydrate C–O–C linkage, respectively.[17,51] Alternatively, NCH showed bands at 3454, 3253, 3105, 2891, 1619, 1553, 1424, and 1004 cm^{-1}, corresponding to the hydroxyl group stretching, NH stretching, CH_3 stretching (symmetric), CH_3 stretching (asymmetric), amide I, amide II, CH_2 bending & deformation and carbohydrate linkage, respectively.[52,53] Meanwhile, the active packaging film without LDHs showed a significant redshift in the OH and CH_3 stretching vibrations, as well as the NH stretching band. On the contrary, the band in the 1600 cm^{-1} region was shifted to the blue area in comparison with the spectra of both neat materials. In addition, the values were recorded in between that of the neat materials with bands at 1416 and 1024 cm^{-1}. In summary, the above-mentioned results confirm the interaction between NALG and NCH at the molecular level. Besides, the addition of LDHs affected the FTIR

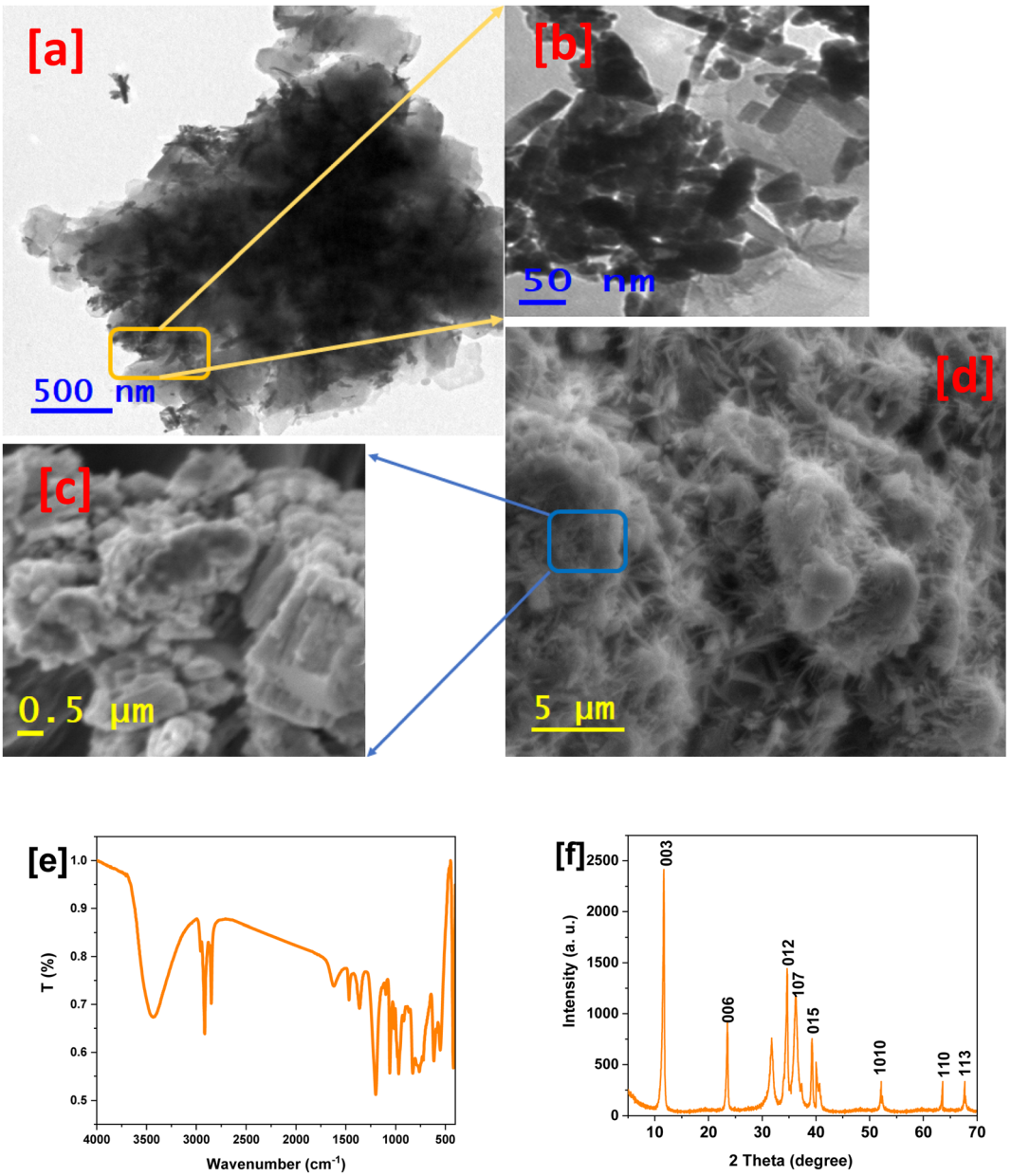

Fig. 1 TEM images of LDHs at low (a) and high magnification (b); SEM images at high (c) and low magnification (d). FTIR spectrum of LDHs (e). XRD pattern of LDHs (f).

spectra of the active packaging films as follows. The low percentage of LDHs added was shown as a blueshift in the bands of OH, CH_3, and C–O–C, with the appearance of a band at 2933 cm^{-1}. Moreover, the characteristic bands of LDHs were recorded at 921, 563, and 420 cm^{-1}. These observations were due to the effect of LDHs on the NALG and NCH helix, such as crosslinking.[54] Indeed, an increase in the content of LDHs affected the behaviour of the functional groups in the FTIR spectra with a significant increase in the intensity of the characteristic bands of LDHs. In other words, the FTIR spectra clearly explained the intermolecular interaction between the active packaging film functional groups and confirmed the formation of a new structure. Herein, the crosslinking mechanism involving LDHs, NALG, and NCH helix could potentially involve numerous steps or interactions. The interaction of LDHs with the NALG and NCH helix may be due to the LDHs being layered structures with positively charged layers and interacting with the negatively charged components such as NALG and NCH helix through electrostatic interactions. Alternatively, it may owing to the adsorption of LDHs onto the surfaces of the NALG and NCH helix due to the attractive forces between the layers of LDHs and the helical structures. Also, the LDHs may swell the interlayer spaces when interacting with the NALG and NCH helix, leading to the expansion of the helical structure. The swelling and interaction can facilitate the formation of crosslinks between the LDH layers and the helical

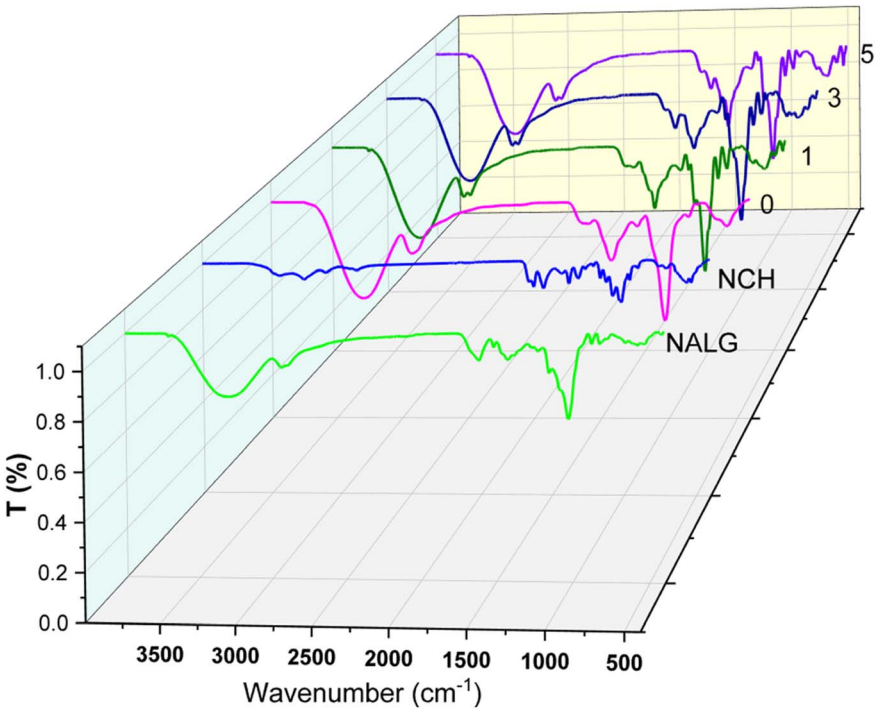

Fig. 2 FTIR spectra of active packaging films and their neat materials.

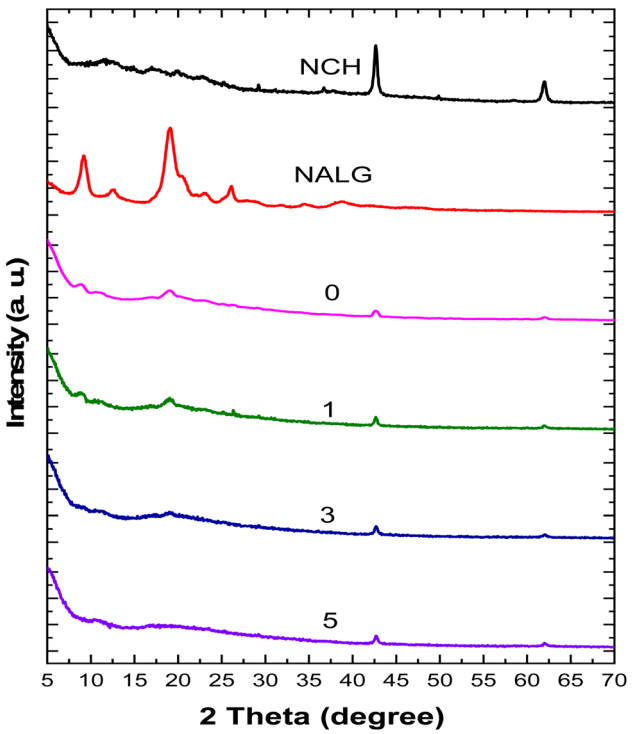

Fig. 3 XRD pattern of active packaging films and their neat materials.

structures, which can stabilize the helix and potentially alter its properties. This suggested mechanism explains how the interaction among LDHs, NALG, and NCH helix can contribute to crosslinking and potentially influence the properties of the prepared nanocomposite material.

The crystallography patterns of the prepared active films and their neat materials are illustrated in Fig. 3. NALG showed peaks at 2θ values of 12°, 17°, 20°, and 23°, which indicate the amorphous and crystal structure of NALG.[55,56] Additionally, the crystallographic pattern of NCH showed peaks at 9.4°, 12.3°, 18.9°, 24°, and 26°, which are in good agreement with other works reporting the mixed amorphous and crystal structure of the α-chitin nanostructure.[57,58] In this context, the pattern of active packaging film without LDHs showed peaks at 9°, 12°, and 20° due to the interaction between NALG and NCH helix, and the same information was extracted from the FTIR data. However, the XDR pattern of the active packaging films containing LDHs showed no significant effect due to the low amount of LDHs as well as the amorphous behaviour of the domain matrix, which affects the XRD pattern more than the crystalline LDHs.

The morphological study of the surface topography of the active packaging films with the absence and presence of different percentages of LDHs is shown in Fig. 4. The free LDH film showed atypical polymer surfaces that were smooth with overlapped areas due to the interaction sites of the NALG and NCH helix, as shown in Fig. 4a. Alternatively, the addition of the LDHs significantly affected the film surface behavior, as shown in Fig. 4b–d. An increase in the ratio of LDHs resulted in an increase in the amount of wrinkles, which confirmed the crosslinking effect of LDHs, as remarked in the FTIR section. Moreover, rods of LDHs that were homogeneously distributed were noted in active packaging film 5.

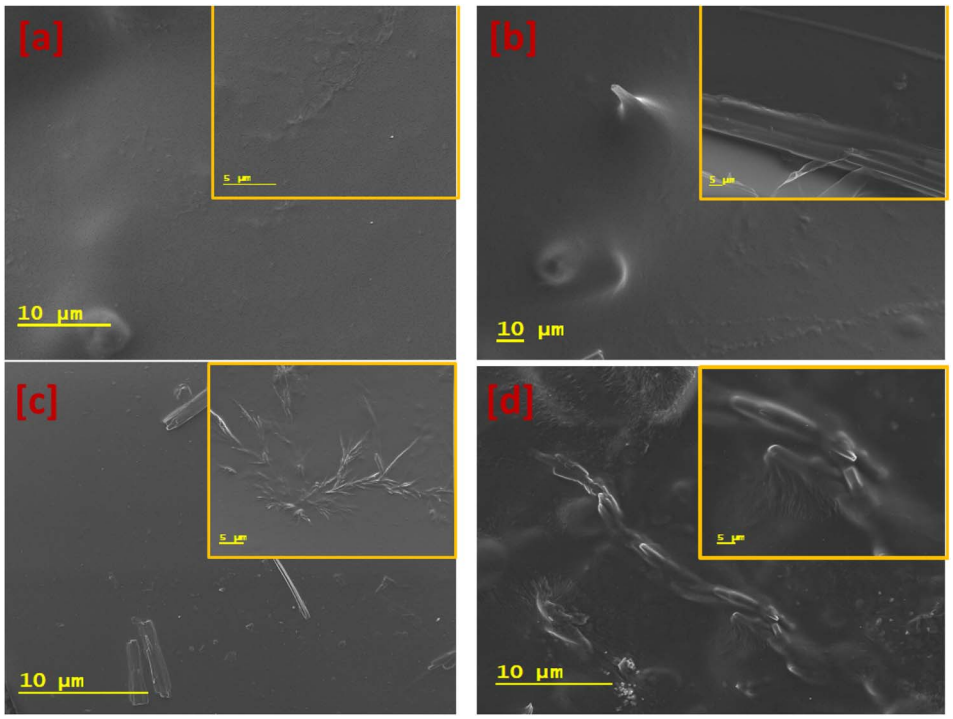

Fig. 4 SEM images of the formulated active packaging films with different concentrations of LDHs of 0, 1%, 3%, and 5% in (a), (b), (c), and (d), respectively.

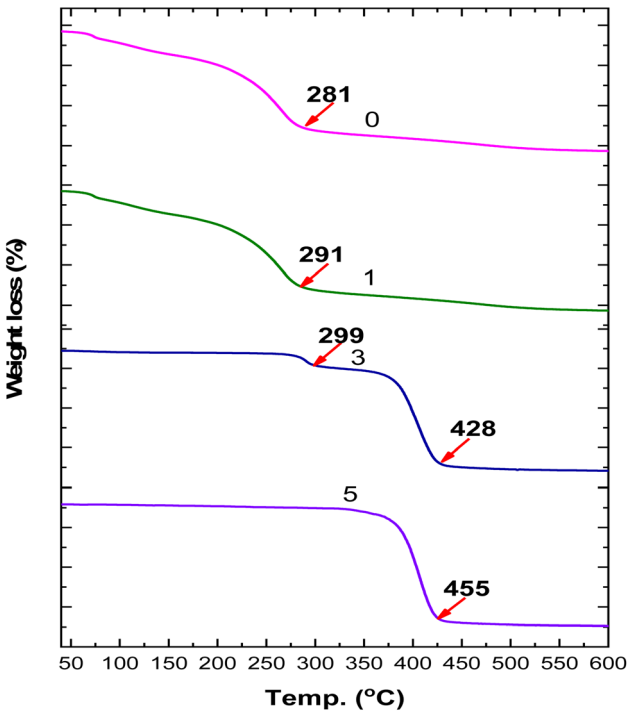

Fig. 5 Thermal analysis of the formulated active packaging films.

The thermal gravimetric analysis (TGA) analysis is illustrated in Fig. 5. The thermal analysis of LDHs demonstrated their high thermal stability in the range 50–600 °C, with weight loss at 600 °C of less than 20% (data not shown). Alternatively, the TGA charts showed the classical behaviors of polysaccharides, which start to decomposed at 281 °C and are destroyed at 550 °C. However, the addition of LDHs enhanced the thermal stability of the active packaging films, as shown in the TGA curve of the film with 0.3% LDHs, where amplification in its decomposition can be observed, which started at 291 °C, whereas that for the film containing the highest percentage of LDHs showed an increase up to 428 °C. This information emphasized a new feature of the prepared active packaging films, *i.e.*, high thermal stability, which could be due to LDHs and their interaction with polysaccharides in the nanoformulation.

Mechanical properties

The mechanical properties of the formulated active packaging were studied and compared with that of the neat NALG. Fig. 6 shows an enhancement in the tensile strength of NALG to 15 MPa, which is a good result in comparison with conventional Na-alginate, as well as good elasticity according to the inverse relationship between deflection and Young's modulus, as reported in previous studies.[59,60] Additionally, the addition of NCH enhanced the tensile strength of NALG by about 47% and its elasticity by about 25%. Otherwise, the addition of LDHs increased the tensile strength by 25% and 41% in active packaging films 1 and 3, respectively, which are acceptable values in comparison with the mechanical properties of biobased polymers[61] and petroleum-based films such as PP polymer films used for packaging purposes.[62] However, active packaging film 5

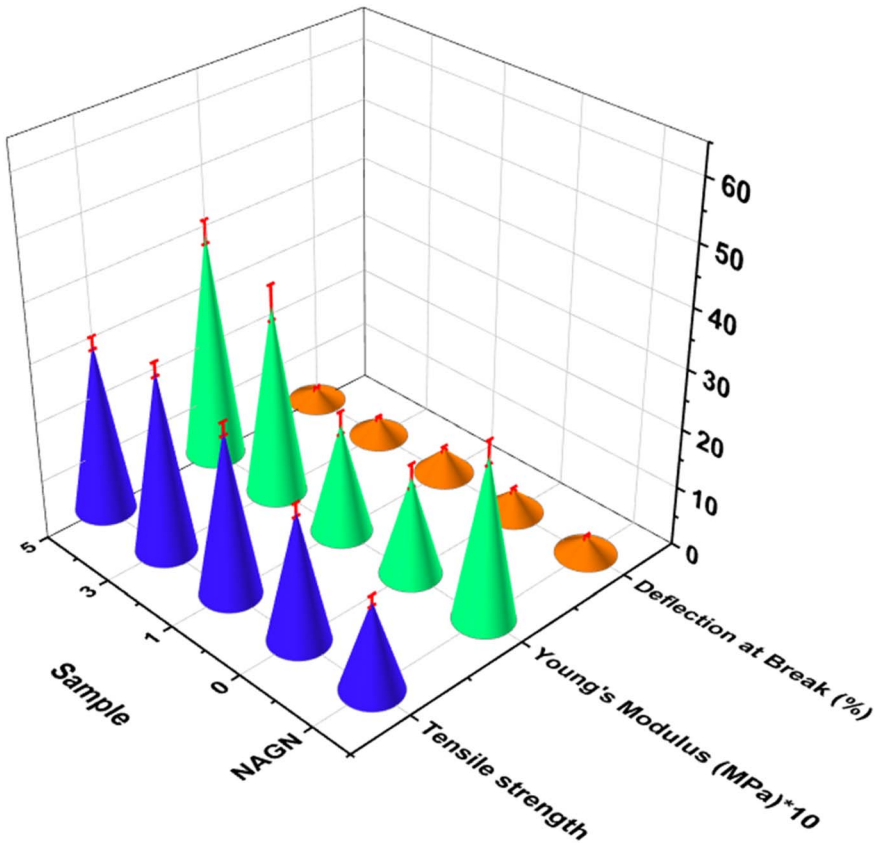

Fig. 6 Mechanical properties of the formulated active packaging films.

was the opposite, with a decrease in its tensile strength, which may be due to the strong cross-linking effect of LDHs at high concentrations, causing the film to become more rigid. This observation was confirmed by the elasticity values, where the deflection decreased by 45%, and Young's modulus increased by about 100%.

Permeability of active packaging films

The oxygen transmission rate (OTR) and the water vapor transmission rate (WVTR) of the formulated active packaging films were investigated using a GBI W303 (B) water vapor permeability analyzer and N530 gas permeability analyzer, respectively. The permeability of oxygen and water vapor is crucial for the materials used in packaging applications, especially food packaging. Therefore, the amount of water vapor and oxygen gas that enters the food, as well as the loss from food to the environment, has a unique effect on the consistency, quality under protection, and shelf life of food. Herein, the obtained data reinforced the acceptable values in comparison with bio-based polymers[63] as well as petroleum-based polymer films used in packaging.[64] The OTR and WVTR values for the formulated active packaging films are shown in Table 1. The obtained results (Table 1) revealed that the formulated active packaging film without LDHs exhibited a greater WVTR than that containing LDHs, which was recorded to be 1870.6 g per m^2 per day. Alternatively, the prepared active packaging films containing LDHs with percentages of 1%, 3%, and 5% w/w were observed to show a decrease in WVTR value from 1870.6 g per m^2 per day to 1640.3, 1380.6, and 860.8 g per m^2 per day, respectively.

Additionally, the OTR is essential given that oxygen is the primary component in the oxidation process, which affects the flavor, odor, and color of food, as well as nutrient degradation.[65]

Table 1 Permeability evaluation of the formulated active packaging films

Samples	Thickness, mm	O_2 TR (g per m^2 per day)	O_2, permeability, g per m^2 per day	WVTR per m^2 per day
0	0.2	70.8 ± 9	7.06×10^{-2}	1870.6 ± 16
1	0.2	50.9 ± 5	5.1×10^{-2}	1640.3 ± 14
3	0.2	38.4 ± 5	3.84×10^{-2}	1380.6 ± 21
5	0.2	24.6 ± 4	2.46×10^{-2}	860.8 ± 17

As a result, the active packaging films containing LDHs offer a sufficient O_2 barrier, which may help improve the quality and increase the shelf-life of food. The oxygen transmission rate (OTR) of the LDH-free active packaging film was 70.8 g per m^2 per day, while the addition of LDHs in various ratios was seen to have the following properties: the OTR of the manufactured active packaging films containing LDHs decreased compared to the LDH-free film with an increase in the loading of LDHs in the active packaging films. With an increase in the presence of LDHs by 1%, 3%, and 5%, the OTR of the synthesized active packaging films containing LDHs was subsequently considerably lowered, with the OTR increasing to 50.9, 38.4, and 24.6 g per m^2 per day, respectively. The results indicated that the active packaging films containing LDHs are promising packaging materials.

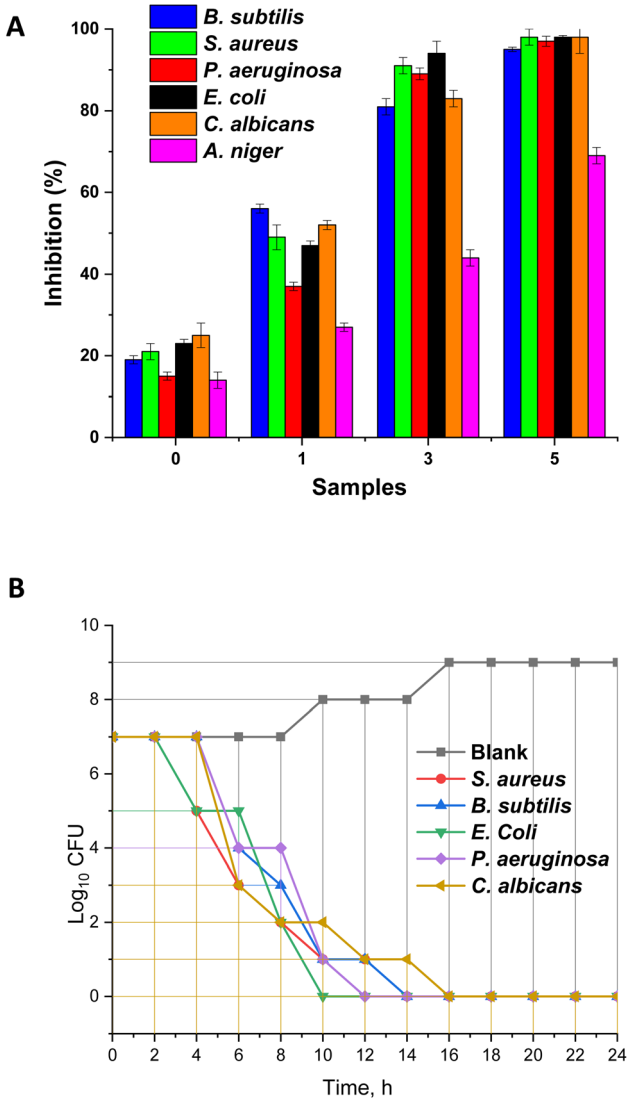

Fig. 7 Antimicrobial activity of formulated packaging films. (A) Antimicrobial activity *via* turbidimetric method (samples 0 (0 LDHs), 1 (1% LDHs), 3 (3% LDHs), and 5 (5% LDHs)) as well as (B) time required for killing by the active packaging film containing 5% of LDHs.

Antimicrobial

The antimicrobial study for the prepared active packaging films tested their ability to reduce the microbial communities affecting the food quality. Fig. 7a illustrates the antimicrobial behavior of the tested active packaging films. The active packaging film without LDHs was observed to have a low antimicrobial activity, which was around 20% inhibition of most of the microbial population used in this test. This activity may be due to chitin, which has limited antimicrobial activity.[66,67] In contrast, the addition of LDHs enhanced the antimicrobial activity, which increased with an increase in the concentration of LDHs. In this context, the 2% and 3% concentrations of LDHs were observed to result in excellent antimicrobial activity, especially against bacterial strains and unicellular fungi, with inhibition of more than 80% and 90%, respectively. The antifungal activity of the active packaging films containing LDHs was relevant, with about 70% inhibition in the highest concentration and less than 50% in concentrations of 1% and 3%. In summary, this observation confirmed the antimicrobial activity of the active packaging films containing LHDs and their moderate antimicrobial activity against filamentous fungi. Indeed, the antifungal activity, especially for filamentous fungi, is usually lacking in antimicrobial agents. However, antimicrobial activity of above 50% inhibition is acceptable in the fungal case given that these robust microorganisms are resistant. Also, the antimicrobial activity of the active packaging films mostly originated from LDHs, which consisted of Al_2O_3 and ZnO,[68,69] and chitin. All the components showed a synergetic effect, which was reflected in the antimicrobial activity. Thus, the bioactive packaging films containing LDHs are described as broad-spectrum antimicrobial packaging films.

In addition, the time required for killing microorganisms was studied for the active packaging film containing a high concentration of LDHs, as presented in Fig. 7b. The growth log showed a high rate of killing of most of the microbial populations, which were deactivated after 12 h. In detail, the *E. coli* and *P. aeruginosa* strains were killed after 8 and 10 h, respectively, while *S. aureus* and *B. subtilis* were killed after 12 h, as well as *C. albicans*. These observations are related to the regular growth rate, which can affect the time required for killing, where the Gram-negative bacteria exhibit fast growth in comparison with Gram-positive bacteria, and *Candida*, depending on the structure of its cell wall is less complicated in Gram-negative and highly complicated in Gram-positive bacteria and *Candida*.

Conclusion

Indeed, the utilization of renewable sources to obtain sustainable products is attractive to satisfy the requirements of environmentally safe policies. In this work, nanostructured active packaging films were successfully formulated based on NALG, which was reinforced with NCH and doped with LDHs in different concentrations. These films were characterized with unique properties and shown to be suitable as food packaging. The formulated active packaging films showed excellent

homogeny at the molecular level, as observed *via* SEM. These formulations possessed a nice physical texture that is acceptable for use as packaging films. Moreover, they exhibited good permeability and mechanical behaviors, as well as antimicrobial activity, which were ascribed to the addition of nanochitin and LDHs. These active packaging films were based on edible and biodegradable biopolymers, which can be biodegraded or consumed by animals to solve the plastic degradation problem and save the environment. Also, the impact of humidity on their barrier properties can be further studied in the future.

Data availability

The data and materials were mentioned in the manuscript and the data was available upon request. The author confirms that the data supporting the findings of this study are available with the corresponding author.

Author contributions

Mohamed S. Hasanin: visualization, methodology, formal analysis, conceptualization, validation, investigation, writing – review, editing. Youssef R. Hassan: visualization, methodology, formal analysis, conceptualization, validation, investigation, review, editing. Ahmed M. Youssef: visualization, methodology, formal analysis, conceptualization, validation, investigation, review, editing.

Conflicts of interest

The authors declare no competing interests.

Acknowledgements

We would like to thank the National Research Centre, Egypt for the possibility to use their facilities. National Research Centre for funding this work under project no. 12020309.

References

1 R. N. Strange and P. R. Scott, Plant disease: a threat to global food security, *Annu. Rev. Phytopathol.*, 2005, **43**, 83–116.
2 S. Bartsch, J. McKinnell, L. Mueller, L. Miller, S. Gohil, S. Huang and B. Lee, Potential economic burden of carbapenem-resistant Enterobacteriaceae (CRE) in the United States, *Clin. Microbiol. Infect.*, 2017, **23**, 48e9–48e16.
3 M. D. Kirk, F. J. Angulo, A. H. Havelaar and R. E. Black, Diarrhoeal disease in children due to contaminated food, *Bull. W. H. O.*, 2017, **95**, 233.
4 N. Elsayed, M. S. Hasanin and M. Abdelraof, Utilization of olive leaves extract coating incorporated with zinc/selenium oxide nanocomposite to improve the postharvest quality of green beans pods, *Bioact. Carbohydr. Diet. Fibre*, 2022, **28**, 100333.
5 M. S. Hasanin and A. M. Youssef, Ecofriendly bioactive film doped CuO nanoparticles based biopolymers and reinforced by enzymatically modified nanocellulose fibers for active packaging applications, *Food Packag. Shelf Life*, 2022, **34**, 100979.
6 S. Ibrahim, H. Elsayed and M. Hasanin, Biodegradable, antimicrobial and antioxidant biofilm for active packaging based on extracted gelatin and lignocelluloses biowastes, *J. Polym. Environ.*, 2021, **29**, 472–482.
7 H. Essawy, A. Badran, A. Youssef and A. E.-F. Abd El-Hakim, Synthesis of poly(methylmethacrylate)/montmorillonite nanocomposites *via in situ* intercalative suspension and emulsion polymerization, *Polym. Bull.*, 2004, **53**, 9–17.
8 A. M. Youssef, F. Malhat, A. A. Hakim and I. Dekany, Synthesis and utilization of poly(methylmethacrylate) nanocomposites based on modified montmorillonite, *Arabian J. Chem.*, 2017, **10**, 631–642.
9 A. F. Ghanem, A. M. Youssef and M. H. Abdel Rehim, Hydrophobically modified graphene oxide as a barrier and antibacterial agent for polystyrene packaging, *J. Mater. Sci.*, 2020, **55**, 4685–4700.
10 N.-A. A. B. Taib, M. R. Rahman, D. Huda, K. K. Kuok, S. Hamdan, M. K. B. Bakri, M. R. M. B. Julaihi and A. Khan, A review on poly lactic acid (PLA) as a biodegradable polymer, *Polym. Bull.*, 2022, 1–35.
11 E. M. Melchor-Martínez, R. Macías-Garbett, L. Alvarado-Ramírez, R. G. Araújo, J. E. Sosa-Hernández, D. Ramírez-Gamboa, L. Parra-Arroyo, A. G. Alvarez, R. P. B. Monteverde and K. A. S. Cazares, Towards a Circular Economy of Plastics: An Evaluation of the Systematic Transition to a New Generation of Bioplastics, *Polym*, 2022, **14**, 1203.
12 M. S. Hasanin, Simple, economic, ecofriendly method to extract starch nanoparticles from potato peel waste for biological applications, *Starke*, 2021, 2100055.
13 M. S. Hasanin, Cellulose-Based Biomaterials: Chemistry and Biomedical Applications, *Starke*, 2022, 2200060.
14 M. Nasrollahzadeh, M. Sajjadi, S. Iravani and R. S. Varma, Starch, cellulose, pectin, gum, alginate, chitin and chitosan derived (nano)materials for sustainable water treatment: A review, *Carbohydr. Polym.*, 2021, **251**, 116986, DOI: **10.1016/j.carbpol.2020.116986**.
15 M. E. El-Naggar, M. Hasanin and A. H. Hashem, Eco-friendly synthesis of superhydrophobic antimicrobial film based on cellulose acetate/polycaprolactone loaded with the green biosynthesized copper nanoparticles for food packaging application, *J. Polym. Environ.*, 2021, 1–13.
16 A. Emamifar and S. Bavaisi, Nanocomposite coating based on sodium alginate and nano-ZnO for extending the storage life of fresh strawberries (Fragaria × ananassa Duch.), *J. Food Meas. Charact.*, 2020, **14**, 1012–1024, DOI: **10.1007/s11694-019-00350-x**.
17 M. Abdelraof, H. El Saied and M. S. Hasanin, Green immobilization of Gluconobacter xylinum onto natural polymers to sustainable bacterial cellulose production, *JWBM*, 2022, **13**, 2053–2069.
18 L. G. Gómez-Mascaraque, M. Martínez-Sanz, S. A. Hogan, A. López-Rubio and A. Brodkorb, Nano- and microstructural evolution of alginate beads in simulated gastrointestinal fluids. Impact of M/G ratio, molecular

weight and pH, *Carbohydr. Polym.*, 2019, **223**, 115121, DOI: 10.1016/j.carbpol.2019.115121.

19 S. Md, S. Abdullah, N. A. Alhakamy, R. A. Shaik, A. R. Ansari, Y. Riadi, J. Ahmad, R. Ali, B. Gorain and S. Karim, Sustained-release ginseng/sodium alginate nano hydrogel formulation, characterization, and *in vivo* assessment to facilitate wound healing, *J. Drug Delivery Sci. Technol.*, 2022, **74**, 103565, DOI: 10.1016/j.jddst.2022.103565.

20 D. Sanjanwala, V. Londhe, R. Trivedi, S. Bonde, S. Sawarkar, V. Kale and V. Patravale, Polysaccharide-based hydrogels for drug delivery and wound management: a review, *Expert Opin Drug Deliv*, 2022, **19**, 1664–1695.

21 S. Lee, L. T. Hao, J. Park, D. X. Oh and D. S. Hwang, Nanochitin and Nanochitosan: Chitin Nanostructure Engineering with Multiscale Properties for Biomedical and Environmental Applications, *Adv. Mater.*, 2023, **35**, 2203325.

22 X. Yang, J. Liu, Y. Pei, X. Zheng and K. Tang, Recent Progress in Preparation and Application of Nano-Chitin Materials, *Int. J. Energy Environ.*, 2020, **3**, 492–515.

23 Z. Li, H. Wang, S. An and X. Yin, Nanochitin whisker enhances insecticidal activity of chemical pesticide for pest insect control and toxicity, *J. Nanobiotechnol.*, 2021, **19**, 49, DOI: 10.1186/s12951-021-00792-w.

24 O. Balayeva, A. Azizov, M. Muradov, R. Alosmanov, S. Zulfugarova, M. Abbasov and S. Mammadyarova, Synthesis Of ZnAL-LDH/PVA Nanocomposite And Adsorption Of Patent Blue V Food Dye From Water Solution, *Azerb. Chem. J.*, 2023, 64–74.

25 Y. Chen, L. Wu, W. Yao, J. Wu, Z. Xie, Y. Yuan, B. Jiang and F. Pan, In situ growth of Mg-Zn-Al LDHs by ZIF-8 carrying Zn source and micro-arc oxidation integrated coating for corrosion and protection of magnesium alloys, *Surf. Coat. Technol.*, 2022, **451**, 129032, DOI: 10.1016/j.surfcoat.2022.129032.

26 S. A. Khan, E. M. Bakhsh, A. M. Asiri and S. B. Khan, Chitosan coated NiAl layered double hydroxide microsphere templated zero-valent metal NPs for environmental remediation, *J. Cleaner Prod.*, 2021, **285**, 124830.

27 G. Gorrasi and V. Bugatti, Mechanical dispersion of layered double hydroxides hosting active molecules in polyethylene: Analysis of structure and physical properties, *Appl. Clay Sci.*, 2016, **132–133**, 2–6, DOI: 10.1016/j.clay.2016.03.011.

28 L. Tammaro, V. Vittoria and V. Bugatti, Dispersion of modified layered double hydroxides in Poly(ethylene terephthalate) by High Energy Ball Milling for food packaging applications, *Eur. Polym. J.*, 2014, **52**, 172–180, DOI: 10.1016/j.eurpolymj.2014.01.001.

29 S. Kumari, S. Soni, A. Sharma, S. Kumar, V. Sharma, V. S. Jaswal, S. K. Bhatia and A. K. Sharma, Layered double hydroxides based composite materials and their applications in food packaging, *Appl. Clay Sci.*, 2024, **247**, 107216.

30 G. Mishra, P. Praharaj, S. Pandey and S. Parida, Biodegradable layered double hydroxide based polymeric films for sustainable food packaging applications, *Appl. Clay Sci.*, 2023, **240**, 106978.

31 X. Cheng, X. Huang, X. Wang and D. Sun, Influence of calcination on the adsorptive removal of phosphate by Zn–Al layered double hydroxides from excess sludge liquor, *J. Hazard. Mater.*, 2010, **177**, 516–523, DOI: 10.1016/j.jhazmat.2009.12.063.

32 A. M. Youssef, H. A. Moustafa, A. Barhoum, A. E.-F. A. A. Hakim and A. Dufresne, Evaluation of the Morphological, Electrical and Antibacterial Properties of Polyaniline Nanocomposite Based on Zn/Al-Layered Double Hydroxides, *ChemistrySelect*, 2017, **2**, 8553–8566, DOI: 10.1002/slct.201701513.

33 J. P. Paques, E. van der Linden, C. J. M. van Rijn and L. M. C. Sagis, Preparation methods of alginate nanoparticles, *Adv. Colloid Interface Sci.*, 2014, **209**, 163–171, DOI: 10.1016/j.cis.2014.03.009.

34 J. P. Paques, L. M. Sagis, C. J. van Rijn and E. van der Linden, Nanospheres of alginate prepared through w/o emulsification and internal gelation with nanoparticles of $CaCO_3$, *Food Hydrocolloids*, 2014, **40**, 182–188.

35 K.-S. Huang, Y.-R. Sheu and I.-C. Chao, Preparation and properties of nanochitosan, *J. Part. Sci. Technol.*, 2009, **48**, 1239–1243.

36 M. S. Hasanin, A. H. Hashem, A. El-Sayed, S. Essam and H. El-Saied, Green ecofriendly bio-deinking of mixed office waste paper using various enzymes from rhizopus microsporus AH_3: efficiency and characteristics, *Cellulose*, 2020, **27**, 4443–4453.

37 M. Abdelraof, M. S. Hasanin, M. M. Farag and H. Y. Ahmed, Green synthesis of bacterial cellulose/bioactive glass nanocomposites: Effect of glass nanoparticles on cellulose yield, biocompatibility and antimicrobial activity, *Int. J. Biol. Macromol.*, 2019, **138**, 975–985, DOI: 10.1016/j.ijbiomac.2019.07.144.

38 R. M. Abdelhameed and M. S. Hasanin, The potential of MOFs embedded in banana cellulose materials for application in dialysis, *J. Mol. Liq.*, 2024, **404**, 124931.

39 S. Dacrory, U. D'Amora, A. Longo, M. S. Hasanin, A. Soriente, I. Fasolino, S. Kamel, M. T. Al-Shemy, L. Ambrosio and S. Scialla, Chitosan/cellulose nanocrystals/graphene oxide scaffolds as a potential pH-responsive wound dressing: Tuning physico-chemical, pro-regenerative and antimicrobial properties, *Int. J. Biol. Macromol.*, 2024, **278**, 134643.

40 I. Eid, M. M. Elsebaei, H. Mohammad, M. Hagras, C. E. Peters, Y. A. Hegazy, B. Cooper, J. Pogliano, K. Pogliano and H. S. Abulkhair, Arylthiazole antibiotics targeting intracellular methicillin-resistant Staphylococcus aureus (MRSA) that interfere with bacterial cell wall synthesis, *Eur. J. Med. Chem.*, 2017, **139**, 665–673.

41 F. Z. Mahjoubi, A. Khalidi, M. Abdennouri and N. Barka, Zn–Al layered double hydroxides intercalated with carbonate, nitrate, chloride and sulphate ions: synthesis, characterisation and dye removal properties, *J. Taibah Univ. Sci*, 2017, **11**, 90–100, DOI: 10.1016/j.jtusci.2015.10.007.

42 A. Elhalil, M. Farnane, A. Machrouhi, F. Z. Mahjoubi, R. Elmoubarki, H. Tounsadi, M. Abdennouri and N. Barka,

Effects of molar ratio and calcination temperature on the adsorption performance of Zn/Al layered double hydroxide nanoparticles in the removal of pharmaceutical pollutants, *J. Sci.: Adv. Mater. Devices*, 2018, **3**, 188–195, DOI: **10.1016/j.jsamd.2018.03.005**.

43 Y. Bai, R. Ma, Z. Jing, X. Wan, J. Tong, W. Huang and J. Liu, Synthesis of Zn/Al layered double hydroxides magnetic-nanoparticle for removal of humic acid, *Desalin. Water Treat.*, 2024, **317**, 100097, DOI: **10.1016/j.dwt.2024.100097**.

44 J. Shin, K. Kim and J. Hong, Zn-Al Layered Double Hydroxide Thin Film Fabricated by the Sputtering Method and Aqueous Solution Treatment, *Coatings*, 2020, **10**, 669.

45 Y. Wei, F. Li and L. Liu, Liquid exfoliation of Zn–Al layered double hydroxide using NaOH/urea aqueous solution at low temperature, *RSC Adv.*, 2014, **4**, 18044–18051.

46 S. Babakhani, Z. A. Talib, M. Z. Hussein and A. A. A. Ahmed, Optical and Thermal Properties of Zn/Al-Layered Double Hydroxide Nanocomposite Intercalated with Sodium Dodecyl Sulfate, *J. Spectrosc.*, 2014, **2014**, 467064, DOI: **10.1155/2014/467064**.

47 M. Rosset, L. W. Sfreddo, O. W. Perez-Lopez and L. A. Féris, Effect of concentration in the equilibrium and kinetics of adsorption of acetylsalicylic acid on ZnAl layered double hydroxide, *J. Environ. Chem. Eng.*, 2020, **8**, 103991, DOI: **10.1016/j.jece.2020.103991**.

48 R. M. A. Q. Jamhour, A. M. Al-Msiedeen, R. Z. Al-Sharaydeh, M. R. Jamhour and A. M. Altweiq, Zn-Al layered double hydroxide nanoparticles for efficient removal of food dyes from wastewater, *Desalin. Water Treat.*, 2024, **317**, 100036, DOI: **10.1016/j.dwt.2024.100036**.

49 J. Liu, J. Song, H. Xiao, L. Zhang, Y. Qin, D. Liu, W. Hou and N. Du, Synthesis and thermal properties of ZnAl layered double hydroxide by urea hydrolysis, *Powder Technol.*, 2014, **253**, 41–45, DOI: **10.1016/j.powtec.2013.11.007**.

50 H. G Fouad, A. S Amin, I. S Ahmed and A. A Ali, Zinc-aluminium layered double hydroxides: Fabrication, study and adsorption application for removal organic dye from aqueous media, *Benha J. Appl. Sci*, 2022, **7**, 53–61.

51 R. Govindaraju, R. Karki, J. Chandrashekarappa, M. Santhanam, A. K. Shankar, H. K. Joshi and G. Divakar, Enhanced water dispersibility of curcumin encapsulated in alginate-polysorbate 80 nano particles and bioavailability in healthy human volunteers, *Pharm. Nanotechnol.*, 2019, **7**, 39–56.

52 C. Chang, N. Peng, M. He, Y. Teramoto, Y. Nishio and L. Zhang, Fabrication and properties of chitin/hydroxyapatite hybrid hydrogels as scaffold nano-materials, *Carbohydr. Polym.*, 2013, **91**, 7–13.

53 M. Kaya, K. Ö. Tozak, T. Baran, G. Sezen and I. Sargin, Natural porous and nano fiber chitin structure from Gammarus argaeus (Gammaridae Crustacea), *EXCLI J.*, 2013, **12**, 503.

54 H. Pang, Y. Wu, Y. Chen, C. Chen, X. Nie, P. Li, G. Huang, Z. P. Xu and F. Y. Han, Development of polysaccharide-coated layered double hydroxide nanocomposites for enhanced oral insulin delivery, *Drug Delivery Transl. Res.*, 2024, **14**, 2345–2355, DOI: **10.1007/s13346-023-01504-7**.

55 H. Helmiyati and K. Wahyuningrum Synthesis and photocatalytic activity of nanocomposite based on sodium alginate from brown algae with ZnO impregnation. in *Proceedings of the AIP Conference Proceedings*, 2018; p. 020107.

56 K. Shalumon, K. Anulekha, S. V. Nair, S. Nair, K. Chennazhi and R. Jayakumar, Sodium alginate/poly (vinyl alcohol)/nano ZnO composite nanofibers for antibacterial wound dressings, *Int. J. Biol. Macromol.*, 2011, **49**, 247–254.

57 M. Kaya, K. Tozak, T. Baran, G. Sezen and I. Sargin, Natural porous and nano fiber chitin structure from Gammarus argaeus (Gammaridae Crustacea), *EXCLI J.*, 2013, **12**, 503–510.

58 D. Cui, J. Yang, B. Lu, L. Deng and H. Shen, Extraction and characterization of chitin from Oratosquilla oratoria shell waste and its application in Brassica campestris L.ssp, *Int. J. Biol. Macromol.*, 2022, **198**, 204–213, DOI: **10.1016/j.ijbiomac.2021.12.173**.

59 G. Zhang, T. Guan, J. Zhang and T. Zhang, Theoretical and experimental investigation of sodium alginate composite films containing star anise ethanol extract/hydroxypropyl-β-cyclodextrin inclusion complex, *J. Food Sci.*, 2021, **86**, 434–442, DOI: **10.1111/1750-3841.15564**.

60 L. Marangoni Júnior, E. Jamróz, S. d. Á. Gonçalves, R. G. da Silva, R. M. V. Alves and R. P. Vieira, Preparation and characterization of sodium alginate films with propolis extract and nano-SiO2, *Food Hydrocolloids Health*, 2022, **2**, 100094, DOI: **10.1016/j.fhfh.2022.100094**.

61 S. Wang, J. K. Muiruri, X. Y. D. Soo, S. Liu, W. Thitsartarn, B. H. Tan, A. Suwardi, Z. Li, Q. Zhu and X. J. Loh, Bio-Polypropylene and Polypropylene-based Biocomposites: Solutions for a Sustainable Future, *Chem.–Asian J.*, 2023, **18**, e202200972.

62 R. A. Khan, M. A. Khan, S. Sultana, M. Nuruzzaman Khan, Q. T. Shubhra and F. G. Noor, Mechanical, degradation, and interfacial properties of synthetic degradable fiber reinforced polypropylene composites, *J. Reinf. Plast. Compos.*, 2010, **29**, 466–476.

63 R. Porta, M. Sabbah and P. Di Pierro, Biopolymers as food packaging materials, *Int. J. Mol. Sci.*, 2020, **21**, 4942.

64 B. M. Trinh, B. P. Chang and T. H. Mekonnen, The barrier properties of sustainable multiphase and multicomponent packaging materials: A review, *Prog. Mater. Sci.*, 2023, **133**, 101071.

65 N. Sruthi, K. Josna, R. Pandiselvam, A. Kothakota, M. Gavahian and A. M. Khaneghah, Impacts of cold plasma treatment on physicochemical, functional, bioactive, textural, and sensory attributes of food: A comprehensive review, *Food Chem.*, 2022, **368**, 130809.

66 M. Benhabiles, R. Salah, H. Lounici, N. Drouiche, M. Goosen and N. Mameri, Antibacterial activity of chitin, chitosan and its oligomers prepared from shrimp shell waste, *Food Hydrocolloids*, 2012, **29**, 48–56.

67 A. Mathur, A. Rawat, G. Bhatt, S. Baweja, F. Ahmad, A. Grover, K. Madhav, M. Dhand, D. Mathur and S. K. Verma, Isolation of Bacillus producing chitinase from soil: production and purification of chito-oligosaccharides

from chitin extracted from fresh water crustaceans and antimicrobial activity of chitinase, *J. Sci. Technol. Res.*, 2011, **3**(11), 1–6.

68 A. M. Baghdadi, A. A. Saddiq, A. Aissa, Y. Algamal and N. M. Khalil, Structural refinement and antimicrobial activity of aluminum oxide nanoparticles, *J. Ceram. Soc. Jpn.*, 2022, **130**, 257–263.

69 D. E. Navarro-Lopez, R. Garcia-Varela, O. Ceballos-Sanchez, A. Sanchez-Martinez, G. Sanchez-Ante, K. Corona-Romero, D. Buentello-Montoya, A. Elias-Zuniga and E. R. Lopez-Mena, Effective antimicrobial activity of ZnO and Yb-doped ZnO nanoparticles against Staphylococcus aureus and Escherichia coli, *Mater. Sci. Eng., C*, 2021, **123**, 112004.